

## 유무기 하이브리드 흡착제의 합성과 수용액에서의 페놀 흡착 특성 연구

Man Yang, Yun Huang<sup>†</sup>, Haijun Cao\*, Yuanhua Lin, Amin Song, and Qingyuan Sun

School of Materials Science and Engineering, Southwest Petroleum University

\*Institute of Blood Transfusion, Chinese Academy of Medical Sciences

(2016년 8월 21일 접수, 2016년 10월 31일 수정, 2016년 11월 30일 채택)

## Synthesis of a Chemically Organic/Inorganic Hybrid Adsorbent and Its Adsorption to Phenol in Aqueous Solution

Man Yang, Yun Huang<sup>†</sup>, Haijun Cao\*, Yuanhua Lin, Amin Song, and Qingyuan Sun

School of Materials Science and Engineering, Southwest Petroleum University, Chengdu, Sichuan Province 610500, PR China

\*Institute of Blood Transfusion, Chinese Academy of Medical Sciences, Chengdu, Sichuan Province 610052, PR China

(Received August 21, 2016; Revised October 31, 2016; Accepted November 30, 2016)

**Abstract:** A novel organic/inorganic hybrid TVE-resin containing SiO<sub>2</sub> structure for phenol removal is successfully prepared by dispersion polymerization, in which the inorganic phase is composed of nano-SiO<sub>2</sub> modified by vinyltrimethoxy silane (VTMS) and the organic phase is constituted of ethylene glycol dimethacrylate (EGDMA). The chemical structure and physical properties of TVE-resin are characterized by FTIR, TGA, SEM and BET. The adsorption studies imply that the novel materials show optimum adsorption capacity at pH=6, dose 0.1 g, contact time 60 min, initial concentration 3000 mg/L and room temperature. The pseudo first-order model can be well fitted with the kinetic process. According to the adsorption isotherm analysis, the Freundlich model gives a better fit to the experimental data, indicating a multiple molecular adsorption for phenol removal. The calculated thermodynamic parameters indicate an exothermic and spontaneous process. A mixture desorption solvent containing methanol and deionized water (v:v, 1:1) can regenerate the TVE-resin completely and the resin displays good reusability after five regeneration recycles.

**Keywords:** adsorption, hybrid, phenol, kinetics, thermodynamics.

### Introduction

Phenol used as one of the most important industrial raw materials is widely applied to plasticizer, pesticides, fungicides, dye, medicine and spices.<sup>1</sup> Owing to its large demand and usage, the ecological system especially the water environment has been suffered a terrible pollution. It can cause the skin and mucous membrane corrosion, inhibit central nervous or damage to the liver and kidney function due to its high toxicity, poor biodegradability and accumulation in the environment.<sup>2</sup> Thus, efficient treatment of phenol-containing wastewater is very urgent for human beings to get healthy drinking water.

In order to remove these phenol-containing effluents, var-

ious methods such as biodegradation,<sup>3</sup> catalytic oxidation,<sup>4</sup> solvent extraction<sup>5</sup> and adsorption<sup>6</sup> have been proposed and developed efficiently. Obviously, adsorption is considered as one of the most promising methods due to the diverse structure, good adsorption capacity and easy regeneration of the adsorbent. Activated carbon acted as a widely used adsorbent exhibits a satisfactory adsorption ability for phenol removal. However, its wider application is restricted due to its high regeneration cost and high attrition rate.<sup>7</sup> Bentonite is a naturally available clay mineral and can be used as a low cost adsorbent, but its relatively poor adsorption capacity needs to be further improved.<sup>8</sup> Polymeric adsorbent containing different kinds of functional groups shows good adsorption ability in organic solvent. While for some water-soluble phenolic pollutants, lower adsorption capacity of these polymeric adsorbents is also inhibited to wide application. The hyper-cross-linked resins such as PDTpc, PDBpc and PGDpc-D<sup>9,10</sup> exhib-

<sup>†</sup>To whom correspondence should be addressed.

E-mail: huangyun982@163.com

©2017 The Polymer Society of Korea. All rights reserved.

ited outstanding adsorption abilities for phenol removal. However, synthesis of these adsorbents is faced with an extremely serious problem: the utilization of recognized carcinogen, chloromethyl methyl ether.

In terms of the above conditions, organic/inorganic hybridized materials including nanoporous structure, crosslinking matrices, sound skeleton strength, and tunable surface chemistry have been paid much attention to phenol removal.<sup>11</sup> Especially, the silicon dioxide nanoparticles containing porous, light and strong adsorption hybridized with polymeric adsorbent have shown the good adsorption capacity and is well worth exploring further.<sup>12</sup> Generally, there are two main manners to attaching polymer chains to silica surface: nano-SiO<sub>2</sub> is physically embedded in the polymeric matrix by weak force.<sup>13</sup> The other is that end-functionalized polymers is chemically bonded to the nano-SiO<sub>2</sub> matrix.<sup>13</sup> The fatal flaw of the first method is that the physically doped nano-SiO<sub>2</sub> can not uniformly disperse in the organic polymeric matrix within a limited scale, which sharply lead to the SiO<sub>2</sub> particle agglomeration and dramatically influence the adsorption capacity.<sup>14</sup> However, the latter can effectively avoid this matter: depended on the covalent attachment, this kind of hybridized material can increase the binding force between nano-SiO<sub>2</sub> particle and organic interface, improve the dispersion ability of nanoparticles, eliminate the surface charge and weaken the surface polarity of particles to gain a good compatibility with polymeric matrix.<sup>15</sup> According to our recent literatures survey,<sup>16-18</sup> the method that siloxane containing carbon-carbon double bond is covalent attachment of nano-SiO<sub>2</sub> particle by dehydration condensation and further copolymerizes with cross-linking agent to achieve the aim of phenol removal, which is still given less concern.

So in this paper, a novel organic/inorganic hybridized adsorbent is prepared. The tetraethoxysilane (TEOS) and vinyltrimethoxy silane (VTMS) are separately used as silicon source and coupling agent. Firstly, VTMS is grafted on the surface of SiO<sub>2</sub> particle to obtain the inorganic phase containing vinyl group. Then, adopting dispersion polymerization, the active SiO<sub>2</sub> particles copolymerize with ethylene glycol dimethacrylate (EGDMA) to obtain the organic/inorganic hybrid TVE-resin. The physical and chemical properties of TVE-resin are characterized by FTIR, TGA, SEM and BET, respectively. The effect of pH, dose, contact time, initial concentration and temperature related on phenol uptake are investigated, which can be further evaluated by adsorption kinetics, isotherms and thermodynamics models. Besides, the regeneration and reusability study of TVE-resin are also discussed.

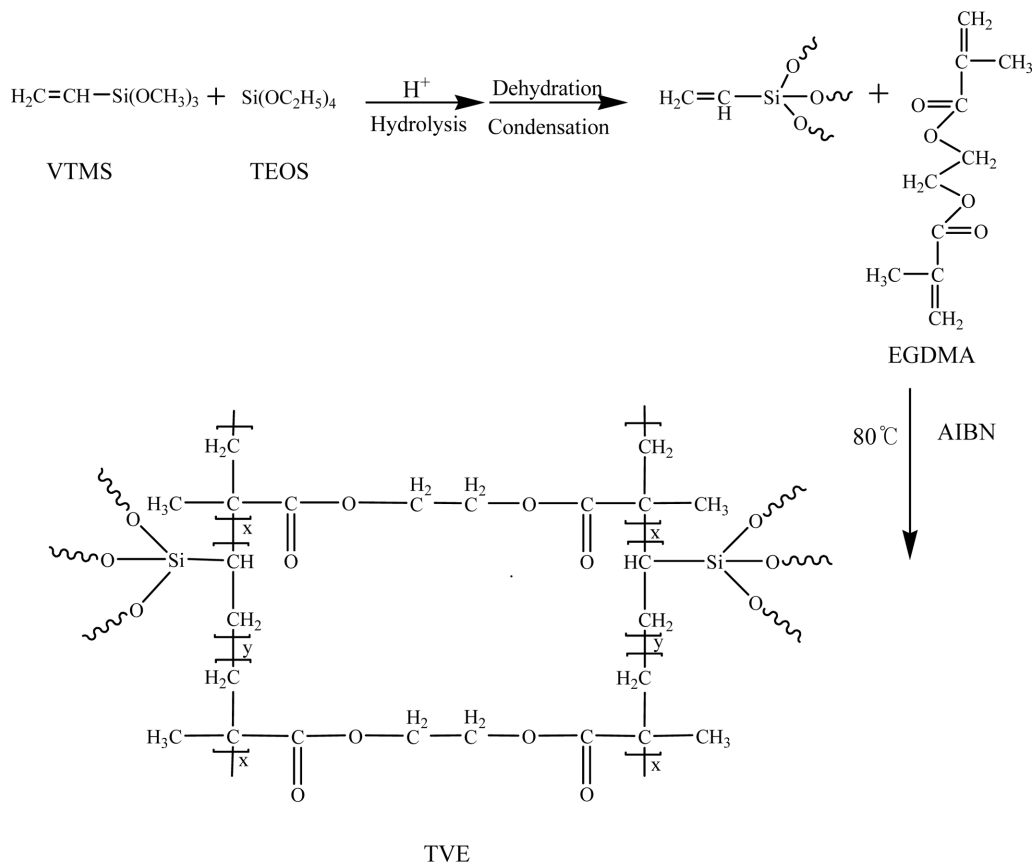
## Experimental

**Materials.** Tetraethoxysilane (TEOS) and vinyltrimethoxy silane (VTMS) were purchased from Nanjing upchemical Co., Ltd. Ethyl acetate, ethanol, methanol, 2,2-azobisisobutyronitrile (AIBN) and phenol were purchased from Kelong Chemical Reagent (Chengdu, China). Ethylene glycol dimethacrylate (EGDMA) employed as cross-linked reagent was obtained from Aladdin Reagent Co., Ltd. Hydrochloric acid and sodium hydroxide applied to adjust the solution pH were obtained from Beijing Chemical Reagent Co., Ltd (Beijing, China). These chemicals were of analytical grade and used without further purification.

**Synthesis of TVE-resin.** The preparation procedure for the TVE-resin was described in Scheme 1. Firstly, 17.8 mL TEOS and 15.3 mL VTMS were added in a mixture of ethanol/water (v:v, 8:1) and adjusted pH=4. The reaction mixture was poured into a three-mouth-flask equipped with a nitrogen inlet, reflux condenser and mechanical stirrer and conducted a co-condensation at 50 °C for 6 h. Then, 40 mL ethyl acetate and 0.56 g AIBN were successively added into the flask after the system was increased to 60 °C in the water bath. Promoting the temperature, 3.85 mL EGDMA was slowly dripped within 0.5 h at 80 °C and further keep copolymerization for 6 h. Finally, the TVE-resin in the form of white particle was respectively washed with methanol, ethanol and deionized water three times and dried in a vacuum oven at 60 °C for 24 h.

**Characterization of TVE-resin.** The TVE-resin was characterized with FTIR (Fourier transform infrared spectroscopy), TGA (thermogravimetric analyzer), SEM (scanning electron microscopy) and nitrogen adsorption-desorption. The FTIR measurement was recorded on a Nicolet 6700 spectrophotometer in the region of 4000-400 cm<sup>-1</sup>, using KBr pellet. TGA was conducted on a METTLER TOLEDO, measured the temperature from 25 to 550 °C at a heating rate of 10 °C/min under N<sub>2</sub> atmosphere. SEM images were carried out on a ZEISS Ultra 55 (ZEISS, Germany), operated under high vacuum conditions, to visualize the morphology and size distribution of the particles. Nitrogen adsorption-desorption isotherms were performed at 77 K on an automatic surface area and porosity analyzer ST-MP-9 (Quantachrome Ins, America). The sample was first degassed at 120 °C for 5 h before adsorption measurements.

**Batch Experiments.** The batch experiment was conducted in a thermostatic shaking incubator by adding 0.1 g of adsorbent into the sealed conical flask containing 25 mL of 1000 mg/



**Scheme 1.** Synthetic procedure of the TVE-resin.

L phenol aqueous solution for 24 h. To examine the influence of solution pH on phenol adsorption by TVE-resin, the initial solution pH was adjusted from 2 to 12 using dilute HCl or NaOH solution. The initial and final phenol concentrations were analyzed by a UV-752 spectrophotometer (Shanghai Yoke Instrument. Co., LTD) at the maximum wavelength 270 nm. The effect of TVE-resin dose on phenol removal was measured by mixing 25 mL of phenol solution with desired doses (0.1-0.6 g) and shaking for 24 h.

Adsorption kinetics were carried out by adding 0.8 g of adsorbent into 200 mL of phenol solution with different initial concentrations (1000, 1500 and 2000 mg/L) and 0.5 mL of phenol solution was sampled at predetermined time intervals. The concentration of residual phenol solution was measured until the adsorption equilibrium was reached and the adsorption capacity at contact time  $t$  was calculated as following<sup>19</sup>:

$$Q_t = \frac{(C_0 - C_t)V}{W} \quad (1)$$

Where  $Q_t$  is the adsorption capacity at contact time  $t$  (mg/g);

$C_0$  and  $C_t$  are the concentration of phenol (mg/L) at initial time and the contact time  $t$ , respectively;  $V$  is the volume of the solution (L) and  $W$  is the dose of resin (dry weight, g).

Adsorption isotherms were determined by mixing 0.1 g of TVE-resin with different initial phenol concentrations (500-3000 mg/L) at a desired temperature (293, 303, and 313 K) until the equilibrium was reached. The equilibrium adsorption capacity was calculated with eq. (2):<sup>19</sup>

$$Q_e = \frac{(C_0 - C_e)V}{W} \quad (2)$$

Where  $Q_e$  is equilibrium adsorption capacity (mg/g);  $C_e$  is the equilibrium concentration of phenol solution (mg/L).

**Regeneration Experiments.** Investigating the regeneration of adsorbent is very essential to the multiple reuses of adsorbent to remove harmful organic pollutants from aqueous system.<sup>20</sup> Firstly, 0.1 g of TVE-resin was mixed with 25 mL of 1000 mg/L phenol aqueous solution for 2 h, then it was separated by filtration and desorbed with 20 mL of various eluents (methanol/deionized water, ethanol/deionized water, sodium

hydroxide/methanol and sodium hydroxide/ethanol) (v:v, 1:1). Finally, the adsorbent was washed with deionized water and reused in the consecutive adsorption-desorption cycles in order to ascertain the best eluent.

## Results and Discussion

**Characterization of TVE-resin.** As shown in Figure 1, the characteristic adsorption peaks derived from the monomers TEOS, VTMS and EGDMA can be observed. The bands appear at  $\sim 3411$  and  $1625\text{ cm}^{-1}$  may be related to the -OH vibration of residual Si-OH and adsorbed water, respectively.<sup>21</sup> The band observed at  $1728\text{ cm}^{-1}$  can be assigned to the -C=O stretching vibration. And the peak at  $1397\text{ cm}^{-1}$  is attributed to the stretching vibration -CH<sub>2</sub>. Besides, the adsorption peaks of characteristic group -Si-O-Si- are easily observed at  $1119$  and  $616\text{ cm}^{-1}$ .<sup>22</sup>

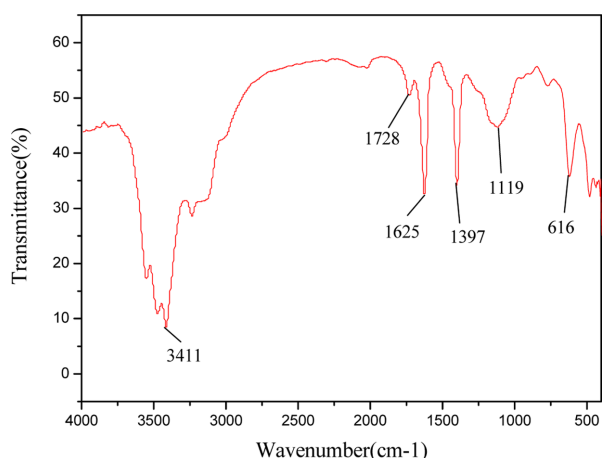


**Figure 1.** FTIR spectrum of the TVE-resin.

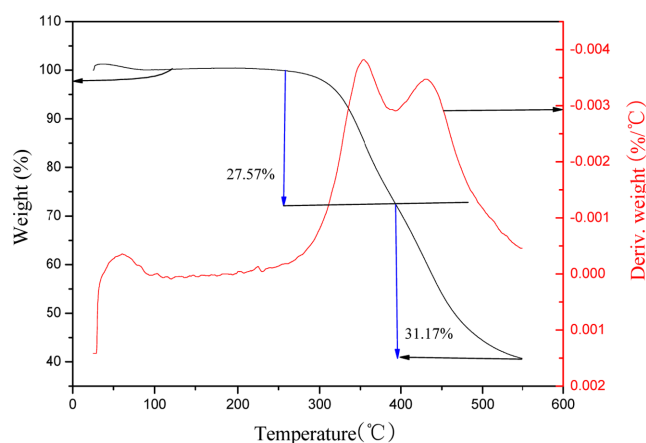


**Figure 2.** Thermogravimetric analysis of the TVE-resin.

Seen from Figure 2, only 1.79% weight of TVE-resin loses before  $259\text{ }^{\circ}\text{C}$ , indicating that the TVE-resin has a high thermal stability. There are two major exothermic peaks in the DTA curve. One is from  $259$  to  $394\text{ }^{\circ}\text{C}$ , and 27.57% of the total weight was lost, which is caused by the rupture of the -C=O, -CH<sub>3</sub> and -CH<sub>2</sub> groups formed some cross-linking chains and fragments on the TVE-resin matrix. The other is from  $394$  to  $550\text{ }^{\circ}\text{C}$ , and 31.17% of total weight was lost, which is attributed to the carbonization of the organic fraction on the TVE-resin.<sup>23</sup> Besides the temperature is over  $550\text{ }^{\circ}\text{C}$ , there is still 41.26% of total weight available, which should be attributed to the existence of the inorganic structure Si-O-Si.

The morphology of TVE-resin is measured by SEM and depicted in Figure 3(a) and (b). The interconnected frameworks of TVE-resin with open porous structure can be found and the rough surface of the particle is also obviously discerned. The porous surface morphology is beneficial to provide active adsorption sites for phenol removal, which should be attributed to the dehydration condensation between siloxane

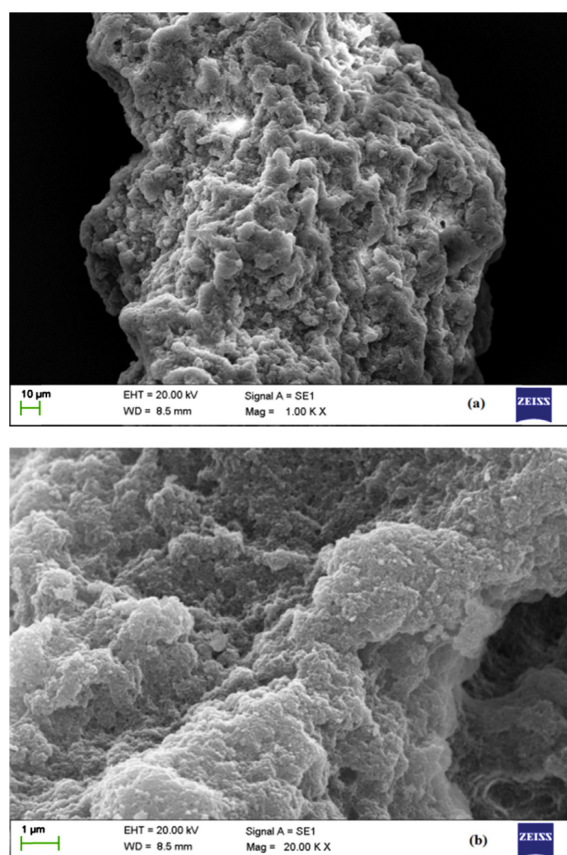


**Figure 3.** SEM images of TVE-resin: (a) low-magnification; (b) high-magnification.

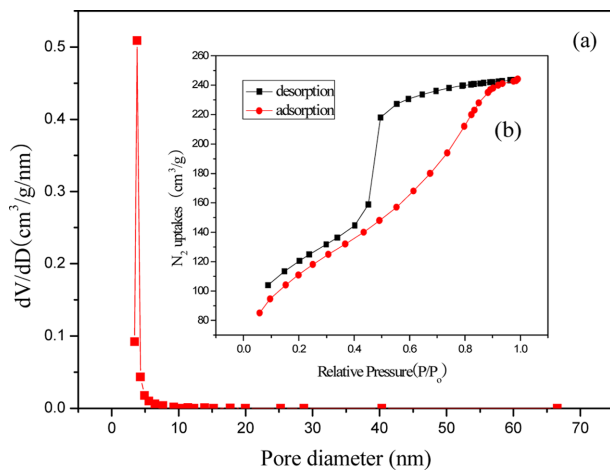


**Figure 4.** (a) BJH desorption pore size distribution of the TVE-resin; (b) nitrogen adsorption-desorption isotherm of the TVE-resin.

**Table 1. Physical Properties of the TVE-resin**

Resin	BET surface area (m <sup>2</sup> /g)	BJH desorption cumulative pore volume (cm <sup>3</sup> /g)	BJH desorption cumulative pore diameter (nm)
TVE-resin	293.9	0.299	3.8

and the cross-linking function of EGDMA. All of these reactions make the TVE-resin constructed in three dimension directions and then presented the stereo network structure.<sup>24</sup>

Figure 4(a) illustrates that mesopore ranged from 3 to 8 nm is predominant and Table 1 exhibits that BJH desorption cumulative pore diameter is 3.8 nm. That is preferential to provide available adsorption channel for phenol molecule transmission. Nitrogen adsorption-desorption isotherm of TVE-resin is displayed in Figure 4(b), which represents a typical type-IV curve with a hysteresis loop in the relative pressure rang 0.4-0.9, reflecting the existence of mesopore again.<sup>25</sup>

**Effect of Solution pH.** The relationship between the adsorption capacity on TVE-resin and the phenol solution pH is determined and the results are depicted in Figure 5. As can be seen from the plot, the adsorption capacity of phenol on TVE-resin is not significantly different at low pH value (2-8). When pH is higher than 8, the phenol uptakes dramatically decrease. It can be explained as that phenol molecules exist in different forms in different pH conditions. The pKa value of phenol is 9.89 and the phenol will be ionized to negative ion when pH > pKa,<sup>26</sup> which leads to an electrostatic repulsion between the residual Si-OH on TVE-resin matrix and the phenolic anion. Besides, the interaction that the hydroxyl bindings

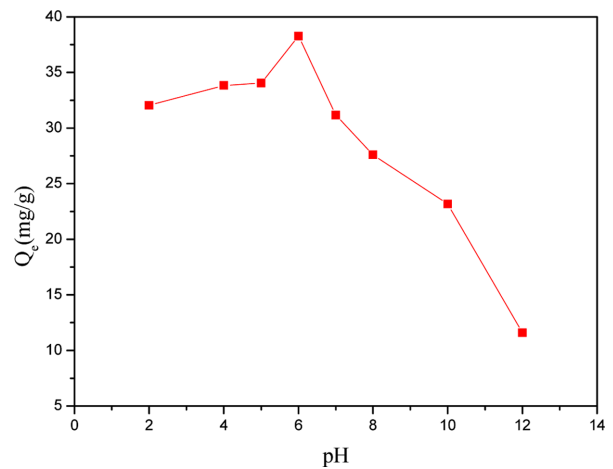


**Figure 5.** Effect of solution pH on phenol uptake by TVE-resin.

formed between phenolic hydroxyl groups and the carbonyl groups on the surface of TVE-resin are played an important role as adsorption driving force to capture the phenol molecules can't exist. All of which results in the extremely low adsorption capacity of phenol.

More definitely, the phenol uptake achieves the largest value and reaches up to 38 mg/g at pH=6 from the Figure 5, which should be attributed to the role of the two kinds of driving forces (hydroxyl binding and van der Waals force).<sup>27</sup> When pH is lower than 6, there are many hydrogen ions H<sup>+</sup> from HCl solution used to adjust pH of phenol aqueous solution, and these H<sup>+</sup> definitely occupy a large number of active adsorption sites on TVE-resin. So the hydroxyl binding interaction between phenol molecules and the functional groups on the TVE-resin matrix will be impaired to some extent. Meanwhile the van der Waals force can continue to afford the phenol removal. Therefore, the optimum adsorption capacity of phenol solution on TVE-resin is pH=6.

In order to imitate the virtual phenol-containing wastewater, the initial pH value of phenol solution is not adjusted and maintained the original value (pH=6) for further studies.

**Effect of TVE-resin Dose.** In attempting to optimize the process of phenol removal, the adsorption capacity of phenol as a function of TVE-resin dose is conducted and the results are displayed in Figure 6. It is observed that increasing the adsorbent dose in the range of 0.1-0.6 g increases the percentage of phenol removal, because the sufficient active adsorption sites and functional groups on the surface of TVE-resin are played a key role in the sorbent-solute interaction.<sup>28</sup> But the equilibrium adsorption capacity  $Q_e$  is found to decrease from 32.05 to 20.18 mg/g. It can be attributed to the insuf-

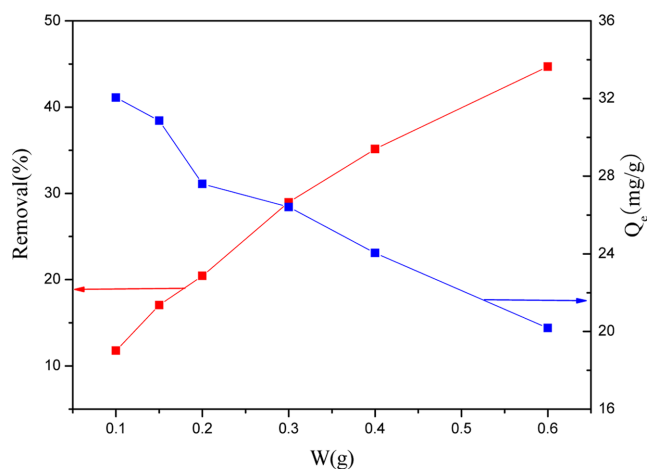


**Figure 6.** Effects of adsorbent dose on removal and phenol uptake by TVE-resin.

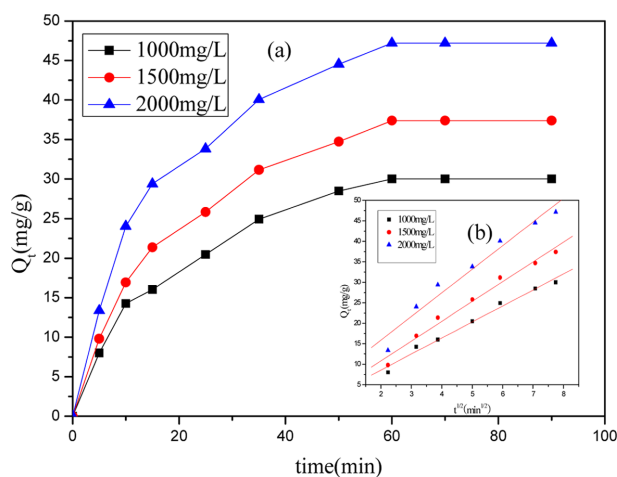


**Figure 7.** (a) Effects of contact time on the adsorption of phenol; (b) fitting results by intra-particle diffusion model.

efficient utilization of active adsorption sites and an increase of the diffusion path length.<sup>29</sup> Because a higher adsorbent concentration will lead to aggregation of TVE-resin particles within a limited volume scales, and as adsorbent doses increased, the aggregation becomes increasingly obvious.

**Adsorption Kinetics.** The adsorption rate of phenol on TVE-resin is characterized by the relationship between adsorption capacity and contact time and the results are shown in Figure 7(a). The ascending trend for phenol uptakes is very obvious within the first 35 min. With time increasing, the trends become slow and the equilibrium reaches at 60 min. At first, a great many active adsorption sites on the surface of TVE-resin can be available for phenol uptakes.<sup>30</sup> Afterward, the adsorption repulsive forces formed between the phenol

molecules adsorbed on TVE-resin and phenol molecules from the aqueous solution are gradually become stronger with time. The adsorption process is eventually reached to the dynamic equilibrium, thereby achieving the equilibrium adsorption capacity.

Obviously, the amount of the phenol uptake increased from 30.00 to 47.19 mg/g as the initial phenol concentration ascended from 1000 to 2000 mg/L. It can be explained as that the concentration distribution of phenol. The larger concentration difference formed between adsorbate and adsorbent is, the more adsorption driving forces obtained. So more phenol molecules can effectively contact with the available adsorption active sites of TVE-resin and further improve the adsorption capacity.

In order to account for the differences of adsorption rate and verify the kinetic models, the pseudo-first-order, the pseudo-second-order and the intra-particle diffusion model equations<sup>31</sup> are all used to fit experiment data and interpret a possible mechanism involved in the adsorption.

The pseudo-first-order and the pseudo-second-order can be expressed by eqs. (3) and (4), respectively.<sup>31</sup>

$$\ln(Q_e - Q_t) = \ln Q_e - k_1 t \quad (3)$$

$$\frac{t}{Q_t} = \frac{1}{k_2 Q_e^2} + \frac{t}{Q_e} \quad (4)$$

Where  $Q_t$  is the amount of phenol adsorbed (mg/g) at contact time  $t$ ;  $Q_e$  is the maximum absorption capacity (mg/g);  $k_1$  ( $\text{min}^{-1}$ ) and  $k_2$  ( $\text{g/mg min}$ ) are separately the pseudo-first-order and pseudo-second-order rate constant for the adsorption process.

The fitting results derived from the linear plots  $\ln(Q_e - Q_t)$  versus  $t$  and  $t/Q_t$  versus  $t$  are listed in Table 2. As can be seen, all of the fitted correlation coefficient values ( $R^2$ ) are found to be greater than 0.98, which shows that the two kinetic models can be applied to predict the adsorption process. However, the other parameter  $Q_e$  shows the different conditions obviously. The  $Q_{e/\text{cal}}$  values at different phenol concentrations by pseudo first-order model are in good agreement with the  $Q_{e/\text{exp}}$  values, but the  $Q_{e/\text{cal}}$  values by pseudo second-order are not close to the experimental values. Judging from the two aspects, the pseudo first-order model is better to predict the entire adsorption process. Besides, analyzing the rate constant obtained from the pseudo first-order, the adsorption rates increase with the initial concentration of phenol increasing, which are once again proved that the larger the concentration difference is, the more

**Table 2. Fitting Results of Adsorption Kinetics of Phenol by TVE-resin**

$C_o$ (mg/L)	$Q_{e/exp}$ (mg/g)	Pseudo-first-order			Pseudo-second-order		
		$Q_{e/cal}$ (mg/g)	$k_1$	$R_1^2$	$Q_{e/cal}$ (mg/g)	$k_2$	$R_2^2$
1000	30.00	29.16	0.048	0.989	39.87	0.00121	0.996
1500	37.40	36.27	0.051	0.997	49.33	0.00100	0.998
2000	47.19	44.52	0.055	0.995	59.56	0.00102	0.998

$Q_{e/exp}$  is the experimental  $Q_e$  and  $Q_{e/cal}$  is the corresponding calculated  $Q_e$  according to the equation under study with best fitted parameters.

**Table 3. Fitting Parameters of Phenol Adsorption on TVE-resin for Intra-particle Diffusion Model**

$C_o$ (mg/L)	Intra-particle diffusion model			
	$Q_i=k_d t^{1/2}+c$	$k_d$	$c$	$R_3^2$
1000	$Q_i=3.916t^{1/2}+0.729$	3.916	0.729	0.993
1500	$Q_i=4.839t^{1/2}+1.113$	4.839	1.113	0.991
2000	$Q_i=5.775t^{1/2}+4.319$	5.775	4.319	0.982

adsorption capacities of phenol on TVE-resin obtain.<sup>32</sup>

Owing to the dimness of the diffusion mechanism, the experimental data are further fitted by the intra-particle diffusion model.<sup>33</sup> It is expressed as following:

$$Q_t = k_d t^{1/2} + c \quad (5)$$

Where  $k_d$  is the intra-particle diffusion rate (mg/g·min<sup>1/2</sup>), and  $c$  is a constant. The  $k_d$  and  $c$  are obtained by plotting  $Q_t$  versus  $t^{1/2}$ .

The fitting results are presented and listed in Figure 7(b) and Table 3, respectively. It is observed that the linear portions of all plots don't pass through the origin, which indicates that intra-particle diffusion is influenced by intra-particle diffusion together with other kinetic effects.<sup>33</sup> According to Table 3, the intercept  $c$  increases from 0.729 to 4.319 with the phenol concentration arranged from 1000 to 2000 mg/L. It can be assigned to increase of the boundary layer thickness, decrease of the external mass transfer and increase of the internal mass transfer.<sup>33</sup>

**Adsorption Isotherms.** The adsorption isotherms of phenol by TVE-resin are illustrated in Figure 8. The higher the temperature is, the less the phenol uptake is, indicating an unfavorable adsorption at high temperature and exothermic process. That has been illustrated by some literatures.<sup>34,35</sup> The specific parameters that express the surface property and the affinity of adsorbent can be plotted by the isotherm model. Both Langmuir and Freundlich adsorption isotherm equations

are the most frequently applied to analyze the equilibrium data.<sup>35</sup>

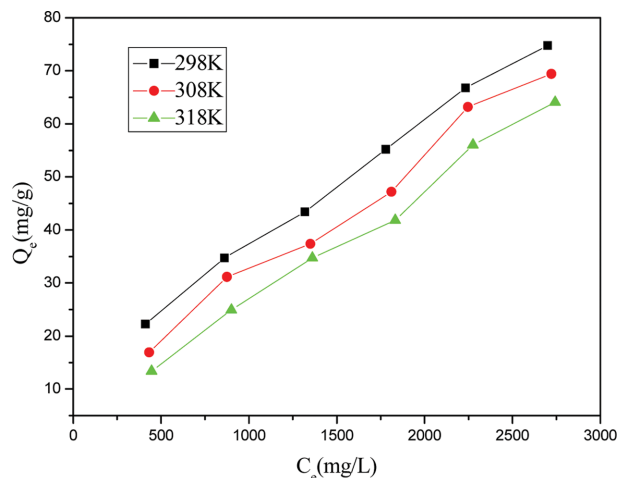
The Langmuir isotherm is used for the monolayer adsorption on a homogenous surface, whereas Freundlich isotherm assumes of non-ideal sorption on heterogeneous surfaces.<sup>35</sup> The linear form of the Langmuir and Freundlich equations are given as following:

$$\text{Langmuir eq.: } \frac{C_e}{Q_e} = \frac{C_e}{Q_m} + \frac{1}{K_L \cdot Q_m} \quad (6)$$

$$\text{Freundlich eq.: } \ln Q_e = \ln K_F + \frac{1}{n} \ln C_e \quad (7)$$

Where  $C_e$  is the residual phenol concentration at equilibrium (mg/L);  $Q_e$  is the equilibrium absorption capacity (mg/g);  $Q_m$  represents a saturated adsorption capacity (mg/g); and  $K_L$  is the Langmuir constant (L/g);  $K_F$  ((mg/g)(mg/L)<sup>1/n</sup>) is the Freundlich constant reflecting the adsorption capacity and  $n$  is the Freundlich exponent representing the adsorption intensity.

The fitting results derived from the plot of  $C_e/Q_e$  versus  $C_e$  and  $\ln Q_e$  versus  $\ln C_e$  are listed in Table 4. As can be seen, the correlation coefficients  $R^2$  in the Freundlich model are over

**Figure 8.** Adsorption isotherms of phenol uptake onto the TVE-resin.

**Table 4. Fitting Parameters of Adsorption Isotherm of Phenol Adsorption at Different Temperatures**

T(K)	Langmuir model			Freundlich model			
	$C_e/Q_e = C_e/Q_m + 1/(K_L \cdot Q_m)$			$\ln Q_e = \ln K_F + (1/n) \ln C_e$			
	$Q_m$	$K_L$	$R^2$	$K_F$	$n$	$R^2$	
298	138.31	0.000401	0.954	0.443	1.547	0.997	
308	171.82	0.000236	0.883	0.172	1.321	0.993	
318	281.69	0.000105	0.764	0.0719	1.168	0.998	

0.99, and the saturated adsorption capacity  $Q_m$  (138.31, 171.82, 281.69 mg/g) by the Langmuir model is separately far away from the experimental values 74.79, 69.4, 64.10 mg/g at 298, 308, 318 K. Besides, the Freundlich constants  $K_F$  and  $n$  decreased with the temperature increase which are in agreement with the exothermic process of phenol uptake, and the values of  $n > 1$  demonstrate a favorable adsorption.<sup>36</sup> All of which indicates that the Freundlich isotherm model can be well employed for fitting the isotherm of phenol uptake on the TVE-resin.

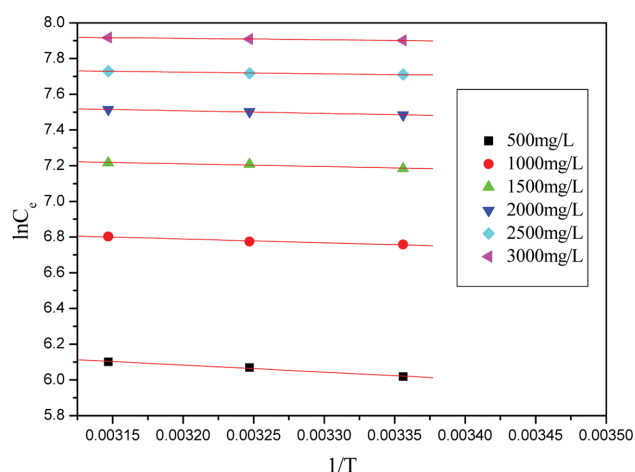
**Adsorption Thermodynamics.** In order to illustrate whether the adsorption process can occur spontaneously or not, the values of thermodynamic parameters including enthalpy change ( $\Delta H$ ), Gibbs free energy ( $\Delta G$ ) and entropy change ( $\Delta S$ ) are determined by the phenol uptakes at different temperatures and obtained from the following eqs. (8)-(10)<sup>37</sup>:

$$\ln C_e = \ln K_o + \frac{\Delta H}{RT} \quad (8)$$

$$\Delta G = -nRT \quad (9)$$

$$\Delta S = \frac{\Delta H - \Delta G}{T} \quad (10)$$

Where  $C_e$  is the equilibrium concentration of phenol (mg/L),  $T$  is the absolute temperature (K),  $\Delta H$  is the isosteric enthalpy change of adsorption (kJ/mol),  $R$  is the ideal gas constant


**Figure 9.** Thermodynamic plots of phenol uptakes at different temperatures.

(8.314 J/mol·K),  $K_o$  is a constant,  $n$  is the Freundlich exponent,  $\Delta G$  is the adsorption free energy (kJ/mol) and  $\Delta S$  is the adsorption entropy change (J/mol·K).

The values of  $\Delta H$  are plotted by  $\ln C_e$  versus  $1/T$  according to Figure 9 and listed in Table 5. It is observed that the negative values of  $\Delta H$  further indicate an exothermic process in nature.<sup>38</sup> By means of the Freundlich exponent  $n$ , the eqs. (9) and (10), the obtained values of  $\Delta G$  and  $\Delta S$  are also listed in Table 5. The absolute values of  $\Delta G$  are 3.83, 3.38, 3.09 at 298, 308, 318 K, respectively, illustrating a spontaneous process

**Table 5. Adsorption Thermodynamic Parameters for the Adsorption of Different Concentrations of Phenol on TVE-resin**

$C_o$ (mg/L)	$\Delta H$ (kJ/mol)	$\Delta G$ (kJ/mol)			$\Delta S$ (J/mol·K)		
		298K	308K	318K	298K	308K	318K
500	-2.91	-3.83	-3.38	-3.09	3.09	1.55	0.57
1000	-1.78				6.88	5.19	4.12
1500	-1.28				8.56	6.82	5.69
2000	-1.19				8.86	7.11	5.97
2500	-0.75				10.34	8.54	7.36
3000	-0.64				10.70	8.90	7.70

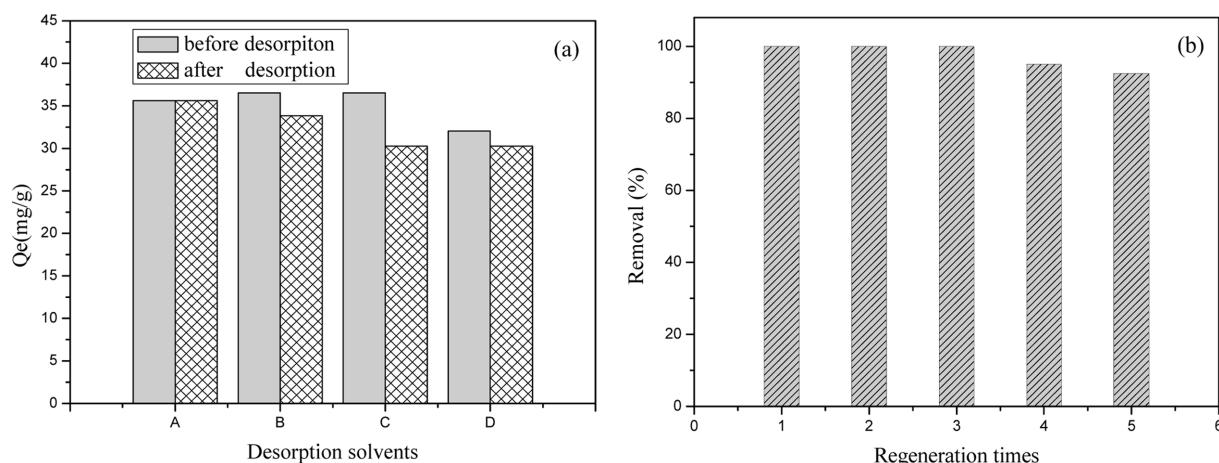


**Figure 10.** (a) Adsorption capacity of phenol on TVE-resin using different solvents (v:v, 1:1) (A: methanol/deionized water; B: ethanol/deionized water; C: 0.1 mol/L sodium hydroxide/methanol; D: 0.1 mol/L sodium hydroxide/ethanol); (b) The effect of regeneration times on recovery ratio of phenol desorption on TVE-resin.

and favorable adsorption at lower temperature. Besides, the positive values of  $\Delta S$  at different temperatures show that the phenol molecules are arranged in a more disorderly manner on the surface of the TVE-resin after adsorption.<sup>38</sup>

**Regeneration and Recyclability.** In order to achieve the best regeneration adsorption capacity, selecting an optimum desorption solvent is very important. The adsorption capacities of phenol before desorption and after on TVE-resin using different solvents are displayed in Figure 10(a). Comparing with the four kinds of mixed desorption solvents, a mixture of methanol and deionized water shows the best desorption ability and then be used to investigate the effect of regeneration time on recovery ratio of phenol desorption. Judging from Figure 10(b), the phenol removal still remains at 92.5% of the initial value after five times of adsorption-desorption process, indicating an excellent reusability and remarkable regeneration. So the TVE-resin can be used as an excellent adsorbent for phenol-containing wastewater removal.

## Conclusions

The hybrid TVE-resin is successfully prepared by dispersion polymerization and can be considered as a potential adsorbent for phenol removal from aqueous solution. The adsorption kinetics analysis implies that the adsorption process reaches equilibrium within 60 min and can be well described by pseudo first-order model. Adsorption isotherm is well represented by the Freundlich model. Thermodynamic analyses reveal that phenol uptake on TVE-resin is an exothermic and

spontaneous process. Besides, the TVE-resin can be regenerated by a mixed desorption solvent containing methanol/deionized water (v:v, 1:1). The results derived from this work are very significant for studying the new purpose of hybrid materials in future.

**Acknowledgement:** The authors gratefully acknowledge the financial support from the Key Fund Project of Sichuan Provincial Department of Education (15ZA0050).

## References

1. M. Anbia and A. Ghaffari, *Appl. Surface Sci.*, **255**, 9487 (2009).
2. F. Q. An and B. G. Gao, *J. Hazard. Mater.*, **152**, 1186 (2008).
3. F. Q. An, R. K. Du, X. H. Wang, M. Wan., X. Dai, and J. F. Gao, *J. Hazard. Mater.*, **201-202**, 74 (2012).
4. G. H. Zhao, Y. F. Li, X. X. Liu, and X. L. Liu, *J. Hazard. Mater.*, **175**, 715 (2010).
5. X. W. Zeng, H. J. Yao, N. Ma, Y. G. Fan, C. H. Wang, and R. F. Shi, *J. Colloid Interface Sci.*, **354**, 353 (2011).
6. T. J. Buran, A. K. Sandhu, Z. Li, C. R. Rock, W. W. Yang, and L. Gu, *J. Food Eng.*, **128**, 167 (2014).
7. J. S. Liu, G. N. Liu, and W. X. Liu, *Chem. Eng. J.*, **257**, 299 (2014).
8. A. Nematollahzadeh, A. Shojaei, and M. Karimi, *React. Funct. Polym.*, **86**, 7 (2015).
9. X. F. Jiang and J. H. Huang, *J. Colloid Interface Sci.*, **467**, 230 (2016).
10. X. Ling, H. B. Li, H. W. Zha, C. L. He, and J. H. Huang, *Chem. Eng. J.*, **286**, 400 (2016).
11. Y. Tian, P. Yin, R. J. Qu, C. H. Wang, H. G. Zheng, and Z. X. Yu, *Chem. Eng. J.*, **162**, 573 (2010).

12. Y. L. Zhao, J. L. Song, D. Wu, T. Tang, and Y. H. Sun, *J. Phys. Chem. Solids*, **86**, 1 (2015).
13. M. E. Parolo, G. R. Pettinari, T. B. Musso, M. P. Sánchez-Izquierdo, and L. G. Fernández, *Appl. Surf. Sci.*, **320**, 356 (2014).
14. C. Y. Jung, J. S. Kim, H. Y. Kim, J. M. Ha, Y. H. Kim, and S. M. Koo, *J. Colloid Interface Sci.*, **367**, 67 (2012).
15. D. Bratkowska, N. Fontanals, F. Borrull, P. A. Cormack, D. C. Sherrington, and R. M. Marce, *J. Chromatogr. A*, **1217**, 3238 (2010).
16. A. G. Kannan, N. R. Choudhury, and N. K. Dutta, *Polymer*, **48**, 7078 (2007).
17. X. Wang, Y. Q. Zheng, C. Y. Zhang, Y. Z. Yang, X. C. Lin, G. H. Huang, and Z. H. Xie, *J. Chromatogr. A*, **1239**, 56 (2012).
18. I. Mallard, L. W. Städe, S. Ruellan, P. A. L. Jacobsen, K. L. Larsen, and S. Fourmentin, *Colloids Surf. A*, **482**, 50 (2015).
19. N. H. Mthombeni, M. S. Onyango, and O. Aoyi, *J. Taiwan Inst. Chem. Eng.*, **50**, 242 (2015).
20. J. X. Han, K. J. Xie, Z. J. Du, W. Zou, and C. Zhang, *Carbohydr. Polym.*, **120**, 85 (2015).
21. E. Durduran, H. Altundag, M. Imamoglu, S. Z. Yildiz, and M. Tuzen, *J. Ind. Eng. Chem.*, **27**, 245 (2015).
22. G. Chang, L. He, W. Zheng, A. Z. Pan, J. Liu, Y. J. Li, and R. J. Cao, *J. Colloid Inter. Sci.*, **396**, 129 (2013).
23. F. X. Zeng, W. J. Liu, S. W. Luo, H. Jiang, H. Q. Yu, and Q. X. Guo, *Ind. Eng. Chem. Res.*, **50**, 11614 (2011).
24. X. M. Wang, M. X. Lu, H. Wang, Y. F. Pei, H. H. Rao, and X. Z. Du, *Separ. Purif. Technol.*, **153**, 7 (2015).
25. Y. H. Kim, B. Lee, K. H. Choo, and S. J. Choi, *Micropor. Mesopor. Mater.*, **185**, 121 (2014).
26. F. Q. An, B. J. Gao, and X. Q. Feng, *Chem. Eng. J.*, **153**, 108 (2009).
27. I. W. Mwangi, J. C. Ngila, P. Ndung'u, and T. A. Msagati, *J. Environ. Manage.*, **134**, 70 (2014).
28. Z. L. Li, Y. Kong, and Y. Y. Ge, *Chem. Eng. J.*, **270**, 229 (2015).
29. B. I. Olu-Owolabi, P. N. Diagboya, and W. C. Ebaddan, *Chem. Eng. J.*, **195-196**, 270 (2012).
30. E. Uguzdogan, E. B. Denkbaz, E. Ozturk, S. A. Tuncel, and O. S. Kabasakal, *J. Hazard. Mater.*, **162**, 1073 (2009).
31. W. Wang, Y. Ma, A. M. Li, Q. Zhou, W. W. Zhou, and J. Jin, *J. Hazard. Mater.*, **294**, 158 (2015).
32. B. K. Sen, D. K. Deshmukh, M. K. Deb, D. Verma, and J. Pal, *Bull. Environ. Contam. Toxicol.*, **93**, 549, (2014).
33. Z. L. Li, Y. Y. Ge, and L. Wan, *J. Hazard. Mater.*, **285**, 77 (2015).
34. Z. Y. Fu, H. B. Li, L. Yang, H. Yuan, Z. H. Jiao, L. M. Chen, J. H. Huang, and Y. N. Liu, *Chem. Eng. J.*, **273**, 240 (2015).
35. X. W. Wu, Y. Liu, Y. F. Liu, and D. L. Di, *Colloids Surf. A*, **469**, 141 (2015).
36. Ł. Klapiszewski, P. Bartczak, M. Wysokowski, M. Jankowska, K. Kabat, and T. Jesionowski, *Chem. Eng. J.*, **260**, 684 (2015).
37. J. H. Huang, K. L. Huang, S. Q. Liu, Q. Luo, and S. Y. Shi, *J. Colloid Interface Sci.*, **317**, 434 (2008).
38. G. D. Yang, L. Tang, G. M. Zeng, Y. Cai, J. Tang, Y. Pang, Y. Zhou, Y. Y. Liu, J. J. Wang, S. Zhang, and W. P. Xiong, *Chem. Eng. J.*, **259**, 854 (2015).